EUROPHYSICS LETTERS 1 June 1992

Europhys. Lett., **19** (3), pp. 155-160 (1992)

Simulating Microscopic Hydrodynamic Phenomena with Dissipative Particle Dynamics.

P. J. HOOGERBRUGGE and J. M. V. A. KOELMAN

Shell Research B.V. - P.O.Box 60, 2280 AB Rijswijk, The Netherlands

(received 19 February 1992; accepted in final form 29 April 1992)

PACS. 02.70 – Computational techniques.
PACS. 51.10 – Kinetic and transport theory.

Abstract. – We present a novel method for simulating hydrodynamic phenomena. This particle-based method combines features from molecular dynamics and lattice-gas automata. It is shown theoretically as well as in simulations that a quantitative description of isothermal Navier-Stokes flow is obtained with relatively few particles. Computationally, the method is much faster than molecular dynamics, and the at same time it is much more flexible than lattice-gas automata schemes.

Predicting complex hydrodynamic behaviour is undoubtedly one of the biggest remaining challenges in classical physics. In dispersed systems such as colloidal suspensions complicated flow behaviours occur even at low Reynolds numbers. The traditional rheological modelling approach, which involves setting up and numerically solving partial differential equations describing the macroscale hydrodynamic behaviour of these complex fluids, has met only limited success. Less traditionally one can—in principle at least—simulate any fluid system rigorously at a microscopic level and make the translation to macroscopic variables in large-scale computer simulations. In the past few years several research groups have reported molecular-dynamics (MD) simulations of flow phenomena occurring in simple fluids, including eddy formation [1] and Rayleigh-Bénard convection [2, 3]. However, even for these simple fluid systems, computational costs limited these studies to 2D systems. Therefore, MD can hardly be considered a tool for studying complex fluids in three dimensions.

A completely new line of approach in particle-based simulations of fluids was triggered by the discovery of Frisch, Hasslacher and Pomeau [4] that systems of particles, moving simultaneously from site to site on a regular lattice, can be tuned into valid fluid-dynamical models yielding the correct Navier-Stokes hydrodynamic behaviour at a coarse-grained scale. These so-called lattice-gas automata (LGA) hold some promise as a practical tool for modelling complex fluid flows, as they are computationally much more efficient than MD. Not only is the number of elementary operations per particle and per time step smaller for LGA, but also, and more importantly, the time steps in LGA are orders of magnitude larger: in a single LGA time step the changes in the relative particle positions are typically comparable to the mean free path of the particles, whereas in MD corresponding changes in local particle configurations usually require hundreds of time steps. Thanks to the increased computational efficiency, LGA models are well suited to simulate complex fluid systems such as colloidal

suspensions [5] and polymer solutions [6], which are characterised by a multiplicity of length scales and which are therefore too computationally intensive to be modelled by MD.

Restricting the particles to move on a regular lattice as in LGA increases the computational efficiency considerably, but at the same time it introduces two fundamental problems in the scheme: isotropy and Galilean invariance are both broken. Frisch *et al.* [4] have shown that both problems can be overcome in the special case of single-phase flows. Anisotropy in the flow behaviour (*i.e.* anisotropic dependence of stress on rate of strain) can be eliminated by choosing a lattice with sufficient rotational symmetry (in two dimensions, for example, a triangular lattice with hexagonal symmetry suffices), and the consequences of Galilean noninvariance for the flow behaviour (*i.e.* unphysical advective terms) can be removed by rescaling the velocities. For dispersed systems and other fluid systems more complex than single-phase fluids, however, these problems show up in a much severer form. For instance, in lattice models of immiscible fluid phases isotropy of the interface dynamics is guaranteed only when isotropy is restored rigorously and not just on a coarse-grained hydrodynamic level. Similar problems apply to Galilean invariance at interfaces.

From a practical point of view, an even more important disadvantage is the fact that LGA lose their appealing simplicity and become quite cumbersome models when going to more complicated fluid systems. This is because the number of possible states per lattice site increases dramatically when new features are added. As a result, the LGA route to—for instance—multi-phase flow simulations in 3D seems hopeless.

In the following we will present a method to overcome these problems. By introducing a LGA-type of time-stepping into MD schemes, we are able to construct stochastic particle models for isothermal fluid systems that are fully isotropic and Galilean invariant but at the same time much faster than MD and very flexible with respect to the addition of model features. We believe this scheme to be useful especially in the field of simulations of dispersed systems, such as colloidal suspensions. It will be shown that for this novel model Navier-Stokes flow behaviour emerges in quite small systems.

The model consists of N particles moving in a continuum domain of volume V. As in MD the system is completely defined by specifying all N positions $\boldsymbol{r}_i$ and momenta $\boldsymbol{p}_i$ ($i = 1, ..., N$). Like LGA, the system is updated in discrete time steps δt consisting of a collision phase followed by a propagation. In the collision phase the momenta are simultaneously updated according to the simple rule

$$\boldsymbol{p}_i' = \boldsymbol{p}_i + \sum_j \Omega_{ij} \boldsymbol{e}_{ij}, \tag{1}$$

where $\boldsymbol{e}_{ij} = (\boldsymbol{r}_i - \boldsymbol{r}_j)/|\boldsymbol{r}_i - \boldsymbol{r}_j|$ is the unit vector pointing from particle j to particle i, and the scalar variable Ω_{ij} specifies the momentum transferred from particle j to particle i. In the propagation phase the particle positions change according to a free propagation:

$$\boldsymbol{r}_i' = \boldsymbol{r}_i + \frac{\delta t}{m_i} \boldsymbol{p}_i', \tag{2}$$

with m_i being the mass of particle i. To be a valid fluid-dynamical model, the above system should satisfy the proper conservation laws and symmetries, and this puts some restrictions on the Ω_{ij}'s. To ensure conservation of linear (and angular) momentum, these momentum transfers should be symmetrical in the particle labels: $\Omega_{ij} = \Omega_{ji}$. We furthermore require that Ω_{ij} depends only on scalar quantities. In so far as these scalar quantities depend on particle configurations and motions, their dependences should be expressed in terms of relative positions and relative velocities. These requirements ensure that the model is fully isotropic and Galilean invariant. In addition, the dynamics is made local by restricting the momentum transfers to pairs with a distance r_c from each other: $\Omega_{ij} = 0$ if $|\boldsymbol{r}_i - \boldsymbol{r}_j| > r_c$. Finally,

momenta should be exchanged in such a way that a homogeneous equilibrium state emerges.

Many different models fitting in the general framework of eqs. (1) and (2) with Ω_{ij} satisfying the above requirements can be defined. Note, however, that thermostated MD schemes like Nosé-Hoover dynamics [7] which are not Galilean invariant and do not conserve local momentum are excluded. Standard MD schemes, though, do fit into our framework. For instance, if Ω_{ij} depends only on $|\boldsymbol{r}_i - \boldsymbol{r}_j|$, the update scheme given by eqs. (1) and (2) reduces to what is essentially the centred-difference MD scheme used by Verlet [8] and others. Here, we will not restrict ourselves to a simple distance dependence; instead, we exploit the fact that, according to the above criteria, Ω_{ij} may also depend on scalars such as $(\boldsymbol{r}_i - \boldsymbol{r}_j) \cdot (\boldsymbol{p}_i/m_i - \boldsymbol{p}_j/m_j)$. We experimented with several different models, but in the following we limit ourselves to one specific model that might not be the optimal model for all computational purposes, but which possesses an appealing conceptual simplicity. Limiting ourselves to systems of particles with equal mass, the expression for Ω_{ij} in this model can be written as

$$\Omega_{ij} = W(|\boldsymbol{r}_i - \boldsymbol{r}_j|)\{\Pi_{ij} - \omega(\boldsymbol{p}_i - \boldsymbol{p}_j)\cdot\boldsymbol{e}_{ij}\}. \tag{3}$$

Here ω is a positive number, and $W(r)$ is a dimensionless, non-negative weight function that vanishes for $r > r_c$ and that is normalised in such a way that $n\int W(r)\,\mathrm{d}\boldsymbol{r} = 1$, where $n = N/V$ is the average particle density in the system. Furthermore, for every pair of particles (i,j), Π_{ij} $(= \Pi_{ji})$ is a random number sampled from a distribution with mean $\langle\Pi_{ij}\rangle = \Pi_0$ and variance $\langle(\Pi_{ij} - \Pi_0)^2\rangle = \delta\Pi^2$.

The important point to note here is that the above specific choice for Ω_{ij} leads to a well-defined equilibrium state. Roughly speaking, the first stochastic term between curly brackets in eq. (3) tends to «heat up» the system, while the second term tends to relax any relative motion (assuming ω is not so large to cause strong over-relaxation). Both terms together act as a thermostat: if the system gets too «hot», the second dampening term (being proportional to the relative motion of the particles) will dominate and cool the system, whereas in too «cold» systems the stochastic term will dominate and drive the system to higher temperatures.

The damping term is primarily responsible for the viscous effects and the stochastic term leads to the correct pressure effects. This can be shown analytically in the continuum limit obtained by increasing the density so that nr_c^d (with $d = 2$ or 3 depending on the number of spatial dimensions) tends to infinity. In this limit the discrete-particle system is described on a coarse-grained level as a continuum, with the momenta $\boldsymbol{p}_i$ being replaced by the field $\boldsymbol{p}(\boldsymbol{r}_i)$ and the local mass density given by $\rho(\boldsymbol{r})$. It follows that, to lowest order in the field gradients, the average coarse-grained dynamics obeys the equations for Navier-Stokes flow with pressure $P = c^2\rho^2/(2\langle\rho\rangle)$, in which the average mass density $\langle\rho\rangle = nm$ and the square of the speed of sound

$$c^2 = \frac{\Pi_0\langle r\rangle}{dm\,\delta t} \tag{4}$$

and with kinematic viscosity

$$\nu = \frac{\omega\langle r^2\rangle}{2d(d+2)\,\delta t}\,. \tag{5}$$

In these equations m denotes the particle mass and the normalized moments of the weight function $W(r)$ are given by $\langle r^k\rangle = n\int r^k W(r)\,\mathrm{d}\boldsymbol{r}$.

We have systematically tested the scheme in two dimensions, and we also did some 3D

simulations. Here, we will focus on the 2D simulations in which we used a simple continuous weight function for $r < r_c$ given by $W(r) = (3/(\pi r_c^2 n))(1 - r/r_c)$. Working in reduced units so that the time step δt, the interaction range r_c and the particle mass m all have a value of unity, we choose $\omega = 4/3$ and obtained $\Pi_0 = 9 \cdot \delta\Pi^2 = 1/3$ by sampling the random numbers Π_{ij} from a uniform distribution between 0 and 2/3. To verify the validity of the model itself, as well as to test the applicability of the continuum approximation, we measured the pressure and the single-particle velocity distribution in a square geometry with periodic boundary conditions. As expected, the velocity distribution matched the Maxwell-Boltzmann distribution perfectly. The match was independent of the average density n, which was varied between 2 and 8. In the same density range we found a perfect agreement with the equation of state: $\langle P \rangle = c^2 \langle \rho \rangle / 2$. The square of the speed of sound was in all cases surprisingly close to the continuum limit value of 1/12. For densities $n = 2$, 4, and 8, we measured (within a 1% error level): $c^2 = 0.0808$, 0.0830 and 0.0838, respectively. Independent measurements of the sound velocity using density perturbations to generate sound waves confirmed these results. The close match of the speed of sound with the continuum limit value already suggests that the correct continuum behaviour in our scheme sets in at length scales comparable to the average nearest-neighbour distance.

We also measured the nondiagonal elements of the pressure tensor in a plane Couette flow profile. To obtain this uniform shearing flow, we used a rectangular geometry with shearing periodic boundary conditions, the so-called Lees-Edwards boundary conditions [9]. In the same density range, $2 \leqslant n \leqslant 8$, we obtained a shear viscosity that was almost independent of the shear rate (which ranged from 0.002 to 0.050). Such a simple Newtonian flow behaviour is not generic for our model; at significantly lower noise levels, obtained by reducing the variance $\delta\Omega^2$, we observed a more complex rheological behaviour with shear viscosities increasing at lower shear rates. In the present case, however, the shear viscosity has a well-defined zero-shear-rate value. For the densities $n = 2$, 4 and 8, we obtained (within a 1% error level): $\nu = 0.0455$, 0.0315 and 0.0280, respectively. Evidently, the viscosity values are less close to the continuum value of 1/40, but they approach this limiting value rapidly with increasing density. Again, we conclude that the continuum limit is quantitatively correct for relatively small length scales. The viscosity measurements were independently confirmed by measuring the $\exp[-k^2 \nu t]$ decay of sinusoidal shear profiles at wave numbers k compatible with the periodic domain. When we performed equilibrium and plane Couette flow experiments in 3D under similar conditions, we also observed the same rapid approach of the values for the speed of sound and the shear viscosity to the continuum-limit values.

As a further validation of the method, and to assess its accuracy in simulating the hydrodynamic interaction between solid particles, we simulated the low Reynolds number flow through a square array of cylinders. To simulate an infinite array of cylinders, these simulations were performed on rectangular domains containing five cylinders in a row with a prescribed pressure difference between the ends of the row. Periodic boundary conditions were used in the lateral direction. The flow velocity and drag force were measured on the central cylinder, the other four cylinders serving to impose on it the inflow and outflow boundary conditions that such a cell would experience in an infinite array. The solid cylinders were implemented in a very direct way corresponding physically to a local «freezing» of the fluid. This is done in a way which does not affect the collision phase: eq. (1) still applies to all particles in the system. However, before the propagation prescription equation (2) is applied, the linear and angular momentum of all «frozen» particles composing a cylinder are summed and redistributed over these particles, so that in the subsequent propagation phase all these particles move together as a rigid object. Notice that in this way, thanks to the dissipative term proportional to ω in eq. (3), stick boundary conditions for the flow originate even in the absence of surface roughness. To prevent the cylinders from rotating and moving with the

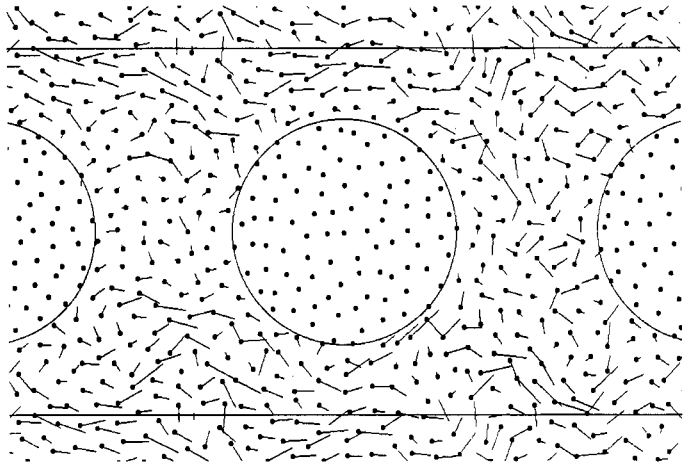

Fig. 1. – Snapshot of particle positions (dots) and displacements during an interval of 20 time steps (straight lines) in a simulation of flow through a square array of cylinders (large circles) with radius $3.7r_c$ occupying 30% of the total volume.

flow (which would result in a simulation of a 2D suspension of hard disks), we held the cylinders at a fixed position and orientation. The force needed to do this was measured and compared with the drag force calculated numerically for square arrays of cylinders [10].

Figure 1 is a «snapshot» of the flow field around the central cylinder with radius 3.7, occupying 30% of the available space. Shown are the instantaneous particle positions (black dots) of all the particles, as well as the moves they make in an interval of 20 time steps (straight lines). Clearly, the particles that define the rigid cylinder distinguish themselves from those in the fluid phase by the absence of any motion. Over the time interval shown, the convective motion of the fluid particles is clearly visible. This is in sharp contrast to MD behaviour where, for the same number of time steps, Brownian motion would dominate. We measured the dimensionless drag (drag force divided by the product of the shear viscosity and the average flow velocity) for solid concentrations of 10% and 30%. For both values of the solid concentration—and for various system sizes—we made several dozen independent

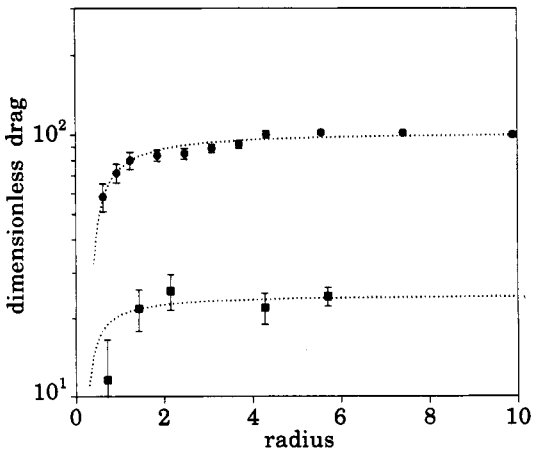

Fig. 2. – Dimensionless drag for creeping flow through a square array of cylinders as a function of cylinder radius (in units r_c) for solid concentration of 10% (solid squares) and 30% (solid circles). Also shown are the results $F_{\text{drag}}(R) = F_{\text{Stokes}}[1 - a/R]$ based on generalised hydrodynamics with fitted values for the length a (dotted curve).

measurements. In order to facilitate comparison with the creeping-flow values for the drag force reported in the literature [10], we limited the pressure difference over the computational domain so that the Reynolds number based on the radius of the cylinders was always below unity. Figure 2 summarises our findings: for both values of the solid concentration, the dimensionless drag forces rapidly approach the values reported in the literature as the system size is increased. This approach towards the Stokes-flow limit is compatible with that expected on the basis of generalised hydrodynamics in 3D [11]: $F_{\text{drag}}(R) = F_{\text{Stokes}}[1 - a/R]$. At a solid concentration of 10% we found $a/c_r = 0.17$. The smallness of the number a/r_c as well as the natural occurrence of stick boundary conditions in our simulation scheme make it possible to obtain quantitatively correct results for very small system sizes. In particular, the values for the drag force are within 10% of the Stokes result for systems as small as that shown in fig. 1, containing a mere 200 fluid particles per unit cell. This number of particles is orders of magnitude lower than the number typically needed in LGA and MD [3] simulations.

We presented a novel particle-based scheme for simulating the dynamics of isothermal fluids. The scheme combines the best of both MD and LGA simulations. The method is much faster than MD and much more flexible than LGA. This increased flexibility was already evident from the ease with which Lees-Edwards boundary conditions and rigid bodies were implemented. Also, with respect to the addition of other features, the method is very flexible. For instance, the scheme can easily be extended to model the (3D) flow of immiscible phases: simply by distinguishing the different fluid phases with different colours and giving the mean Π_0 of the stochastic term in eq. (3) a larger value when particles of different colours interact, phase separation between the fluids can be obtained. Results with simulations of this type will be reported on in the near future.

In conclusion, we think that the present method shows much promise in the simulation of the hydrodynamic behaviour of systems too complicated to be tackled by traditional methods, especially in the field of microscale hydrodynamic phenomena where Brownian effects play a role.

REFERENCES

[1] RAPAPORT D. C. and CLEMENTI E., *Phys. Rev. Lett.*, **57** (1986) 695.
[2] MARESCHAL M. and KESTEMONTE., *Nature*, **329** (1987) 427; MARESCHAL M., MANSOUR M. M., PUHL A. and KESTEMONT E., *Phys. Rev. Lett.*, **61** (1988) 2550.
[3] RAPAPORT D. C., *Phys. Rev. Lett.*, **60** (1988) 2480.
[4] FRISCH U., HASSLACHER B. and POMEAU Y., *Phys. Rev. Lett.*, **56** (1986) 1505.
[5] LADD A. J. C., COLVIN M. E. and FRENKEL D., *Phys. Rev. Lett.*, **60** (1988) 975.
[6] KOELMAN J. M. V. A., *Phys. Rev. Lett.*, **64** (1990) 1915.
[7] HOOVER W. G., *Phys. Rev. A*, **31** (1985) 1695.
[8] VERLET L., *Phys. Rev.*, **159** (1967) 98.
[9] LEES A. W. and EDWARDS S. F., *J. Phys. C*, **5** (1972) 1921.
[10] SANGANI A. S. and ACRIVOS A., *Int. J. Multiphase Flow*, **8** (1982) 193.
[11] ALLEY W. E. and ALDER B. J., *Phys. Rev. A*, **27** (1983) 3158.